

Orbits of Twelve Multiple Stars

ANDREI TOKOVININ¹

¹*Cerro Tololo Inter-American Observatory, NSF's NOIRLab Casilla 603, La Serena, Chile*

ABSTRACT

Inner and outer orbits in twelve hierarchical stellar systems are determined using high-resolution speckle imaging, radial velocities, or both. Masses and fluxes of the components are estimated. The Hipparcos numbers of the main stars are 7111, 12912, 17895, 20375, 42424, 68717, 77439, 79076, 90253, 97922, and 102855; the faint triple WDS J10367+1522 has no HIP number. Four systems are quadruple of 3+1 hierarchy, the rest are triple. Two triples with low-mass M-type components are approximately planar, with moderately eccentric orbits and near-unit mass ratios. The shortest inner period of 0.27d is found in the newly identified contact eclipsing pair belonging to the misaligned quadruple HIP 97922. The compact system HIP 102855 (periods 15.4 and 129 days) identified by Gaia is confirmed here and has additional companion at 6''. This work contributes new data for the study of diverse architectures of stellar hierarchies in the field.

1. INTRODUCTION

This paper reports on the orbital parameters and masses in several hierarchical stellar systems, deduced from original observations. It is an incremental contribution to the collection of data on stellar hierarchies in the Multiple Star Catalog, MSC (A. Tokovinin 2018a).²

Bound systems of three or more stars are relics of star formation, and their architecture (masses, periods, eccentricities, mutual orbit orientation) contains valuable information on the origin of stars and planets, both statistically and individually. The statistics of stellar hierarchies, poorly known at present, are also a starting point for modeling their evolution which produces unusual stellar remnants and high-energy events (S. Toonen et al. 2020). Simplistic attempts to model the population of triple systems as independent combinations of two binaries drawn from a common distribution and filtered by dynamical stability (e.g. D. Fabrycky & S. Tremaine 2007) are caused by the lack of actual data. Indeed, owing to the vast range of periods, a relatively complete volume-limited sample of hierarchies exists only for the well-studied nearest solar-type stars (D. Raghavan et al. 2010), and it is necessarily small (56 systems). Extending the distance limit to 67 pc reveals a patchy and incomplete coverage of the parameter space (A. Tokovinin 2014).

A long-term program of monitoring radial velocities (RVs) of late-type stars in hierarchical systems (mostly within 67 pc) in order to determine unknown inner periods has been started by the author in 2015; it contributed \sim 100 spectroscopic orbits and discovered additional, previously unsuspected subsystems (A. Tokovinin 2023). After termination of the project, some stars still lacked spectroscopic orbits, prompting continued observation. Results on one such system, HIP 68717, are published here. This work also revealed that the latest Gaia catalog of non-single stars, NSS (Gaia Collaboration et al. 2023), covers only a third of our sample. Furthermore, not all orbits in the NSS are correct (B. Holl et al. 2023; A. Tokovinin 2025a). This is understandable because signals from multiple systems are often non-trivial and unsuitable for automatic pipelines such as Gaia.

The situation is even less satisfactory in the period range from decades to millenia, where the RV monitoring lacks time coverage, while the all-sky Gaia data lack both spatial resolution and time coverage. High-resolution imaging of binary stars by speckle interferometry at the the 4.1 m SOAR (Southern Astrophysical Research) telescope produced hundreds of serendipitous discoveries of hierarchical systems by resolving inner subsystems in known binaries or by detecting their tertiary companions. For nearby stars, the diffraction-limited resolution of 30 mas gives access to relatively short orbital periods, allowing calculation of orbits: the inner one and, when historic data are available, the outer one as well. Accumulation of speckle data enables a detailed analysis of the system's architecture (see

² The latest MSC versions are available at <https://www.ctio.noirlab.edu/~atokovin/stars> and <http://vizier.u-strasbg.fr/viz-bin/VizieR-4?-source=J/ApJS/235/6>.

A. Tokovinin 2025b, and references therein). Measurements of the mutual orbit inclination are of particular interest for studying the origin of stellar hierarchies and their dynamical evolution (A. Tokovinin 2021a). This paper continues the series based on the SOAR speckle data. Thus, it combines the speckle and RV work.

The basic data on the 12 hierarchies studied here are assembled in Table 1. The systems are identified by the Washington Double Stars (WDS) codes based on the J2000 positions (B. D. Mason et al. 2001) and by numbers of their components in the Hipparcos and HD catalogs. The spectral types and photometry are copied from Simbad, the proper motions (PMs) and parallaxes are, mostly, from the Gaia data release 3 (GDR3) (Gaia Collaboration et al. 2021), and most RVs are from this work. Each hierarchy is discussed individually in the following sections. To give an overall view of their parameters, Table 2 lists the number of known components N and the hierarchy in the bracket notation, where for each pair the primary and secondary masses m_1 and m_2 and the orbital period P are listed. There are 8 triples and 4 quadruples. All quadruples have a 3-tier (3+1) hierarchy (a close inner pair, an intermediate pair, and an outer companion). The orbital periods range from 0.27 days to \sim 200 kyr.

The observational data and methods are briefly introduced in Section 2. Sections 3 to 14 are devoted to individual systems, Section 15 contains the summary.

2. DATA AND METHODS

The input data and their interpretation are similar to the previous papers of this series. Below they are outlined very briefly, with details in the references. The availability of position measurements and RVs and their time coverage differ in each case. Additionally, astrometry and photometry are used to characterize each hierarchy as completely as possible. For this reason, the discussion of individual systems below might appear difficult to grasp and overloaded with numbers such as mass estimates.

2.1. Speckle Interferometry

This work is based on the long-term monitoring of binary and multiple stars with high angular resolution using speckle interferometry at the the 4.1 m SOAR telescope located in Chile. The instrument (high-resolution camera), the data processing, and the performance are covered in A. Tokovinin et al. (2010); A. Tokovinin (2018b). The latest series of measurements and references to prior observations can be found in A. Tokovinin et al. (2024). The cubes of short-exposure images are recorded in the y (543/22 nm) or

I (824/170 nm) filters. The pixel scale (15 mas) and orientation are calibrated using a set of binaries with separations on the order of 1" and accurately modeled motions. Typical external errors of 2 mas and less are achieved, resulting in the most accurate and internally consistent set of speckle data available to date. This is essential for detecting small perturbations (wobble) caused by inner subsystems. Two triples studied here were originally used as calibrators until the wobble was revealed. The measurements (separation, position angle, and magnitude difference) are obtained by fitting models of binary or triple point sources to the speckle power spectra, using single reference stars where necessary to reduce instrumental signatures.

2.2. Radial Velocities

High-resolution optical spectra were taken with the CHIRON echelle spectrometer at the 1.5 m telescope located at Cerro Tololo (A. Tokovinin et al. 2013) and operated by the SMARTS consortium.³ The spectra with a resolution of 80,000 were processed by the instrument pipeline (L. A. Paredes et al. 2021) and cross-correlated with a binary mask based on the solar spectrum (A. Tokovinin 2016). The dips in the cross-correlation function (CCF) inform us on the RVs, while their amplitudes and widths help to estimate relative fluxes and the projected axial rotation $V \sin i$.

2.3. Space Astrometry

The knowledge of parallaxes measured by the Hipparcos (F. van Leeuwen 2007) and Gaia (Gaia Collaboration et al. 2016, 2021) missions is critical for interpretation of the observations. It allows us to convert the fluxes of individual components (determined by distributing the combined flux of an unresolved system between its components using flux ratios deduced from the differential speckle photometry or CCF parameters) into absolute magnitudes and estimate masses via standard relations (M. J. Pecaut & E. E. Mamajek 2013) or isochrones (A. Bressan et al. 2012). Such masses are called here *photometric* to distinguish them from directly measured (“orbital”) masses.

It is well known that astrometry of unresolved multiple systems is often biased (B. Holl et al. 2023). The influence of unresolved subsystems can be gauged by the reduced unit weight error (RUWE) in Gaia or by the proper motion anomaly, PMA (T. D. Brandt 2018, 2021). Luckily, some triples have wide companions with

³ SMARTS stands for Small and Moderate Aperture Research Telescope System, <https://www.astro.gsu.edu/~themy/SMARTS/>

Table 1. Basic Parameters of Observed Multiple Systems

WDS	Comp.	HIP	HD	Spectral	<i>V</i>	<i>V</i> − <i>K_s</i>	μ_{α}^*	μ_{δ}	RV	ϖ^a
(J2000)				Type	(mag)	(mag)	(mas yr ^{−1})	(km s ^{−1})	(mas)	
01316−5322	AB	7111	9438	F5V	7.87	1.30	86	29	29.0	9.72: DR3
	C	11.20	2.03	81	30	31.2	9.68 DR3
02460−0457	AB	12912	17251	F3V	7.52	1.14	56	7	...	10.69 DR3
03496−0220	AB	17895	24031	F8V	7.23	1.48	−59	−41	6.0	19.63 HIP
04218−2146	A	20375	27723	G0V	7.54	1.28	86*	−11*	−3.7	18.99 DR3
	B	20.24	7.42	85	−12	...	18.84 DR3
08391−5557	ABC	42424	74045	F3V	7.46	1.12	−16	6	26.8:	6.22 DR3
10367+1522	AB	M4.0V	13.31	5.41	110	−78	...	50.0 DR3
14040−4437	AB	68717	122613	G1V	8.28	1.86	−9*	−16*	−3.3	11.76 HIP
	C	12.43	3.37	−13	−20	−1.3	12.56 DR3
15474−1054	AB	77349	...	M2.5V	11.28	4.54	−309	−370	3.0	62.52 DR2
16161−3037	AB	79706	146177	F0	7.74	1.12	−26	−21	...	6.20 DR3
18250−0135	AB	90253	169493	F2V	6.19	1.05	5	−3	−12.1	7.49 DR2
19540+1518	A	97922	188328	F8III	7.20	1.57	0	−12	3.9	11.78 DR3
	B	8.65	...	−18	−15	...	11.47 DR3
20503−7502	A	102855	197324	F7V	8.42	1.21	22	−64	15.1	8.29 DR3N
	B	16.63	4.63	23	−67	...	8.12 DR3

Proper motions and parallaxes are from Gaia DR3 ([Gaia Collaboration et al. 2021](#)) or Hipparcos ([F. van Leeuwen 2007](#)). Colons mark parallaxes biased by subsystems, asterisks mark PMs from [T. D. Brandt \(2021\)](#).

Table 2. Masses, Periods, and Hierarchy

WDS	HIP	<i>N</i>	Hierarchy	Masses and Periods	
				$(m_1, m_2; P)$	
01316−5322	7111	4	(A,(Ba,Bb)),C	((1.37,(1.23,0.92; 4.9yr); 285yr),0.83; \sim 126kyr)	
02460−0457	12912	3	A,(Ba,Bb)	(1.41,(1.1,0.58; 38yr); 1kyr)	
03496−0220	17895	3	A,(Ba,Bb)	(1.14,(0.98,0.84; 250d); 47yr)	
04218−2146	20375	3	(Aa,Ab),B	((1.20,0.44; 12.4yr); \sim 194kyr)	
08391−5557	42424	3	A,(B,C)	(1.92,(1.1481.08; 23.5yr); 1.1kyr)	
10367+1522	...	3	A,(B,C)	(0.29,(0.17,0.17; 8.6yr); 120yr)	
14040−4437	68717	4/5	((Aa,Ab),B),(C,?)	(((0.99,0.93; 24d),1.04; 414yr),(0.69+?); \sim 8kyr)	
15474−1054	77349	3	A,(Ba,Bb)	(0.41,(0.23,0.21; 133d); 8.3yr)	
16161−3037	79706	3	(Aa,Ab),B	((1.67,1.21; 7.5yr),1.34; 167yr)	
18250−0135	90253	3	(Aa,Ab),B	((2.28,1.59; 11.75yr),1.96; 386yr)	
19540+1518	97922	4	(Aa,(Ab1,Ab2)),B	((1.34,(1.00,0.30; 0.27d); 68yr),1.12; 3.1kyr)	
20503−7502	102855	4	((Aa1,Aa2),Ab),B	(((1.31,1.06; 15.4d),0.16; 129d),0.38; \sim 11kyr)	

unbiased parallaxes, furnishing accurate distances. Orbits and photometric masses offer additional check of the parallaxes; alternatively, the knowledge of parallaxes and masses helps with poorly constrained orbits.

When a close pair is not resolved directly, its semi-major axis is estimated from the period, mass sum, and parallax using the third Kepler’s law. This helps to interpret the astrometric wobble. A similar approach is used to estimate periods of wide pairs from their projected separations, assuming that they equal the semi-major axes (which is true in the statistical sense). Such

crudely estimated long periods are denoted as P^* , and the actually measured periods as P .

2.4. Orbit Calculation

An IDL code `orbit3` that fits simultaneously inner and outer orbits in a triple system to available position measurements and/or RVs has been used ([A. Tokovinin 2017](#)).⁴ The method is presented in [A. Tokovinin & D. W. Latham \(2017\)](#). The weights are

⁴ Codebase: <http://dx.doi.org/10.5281/zenodo.321854>

inversely proportional to the squares of adopted measurement errors which range from 2 mas to $0''.05$ and more (see A. Tokovinin 2021b, 2024, for further discussion of weighting).

The observed motion in a triple system can be represented by two Keplerian orbits, neglecting mutual perturbations. The relative positions are measured between stars, hence the outer positions include a contribution from the inner pair (wobble). Its amplitude equals the inner semimajor axis multiplied by the wobble factor $|f| = q_{\text{in}}/(1 + q_{\text{in}})$ when the inner pair is resolved, or, otherwise, by the photocenter wobble factor $|f^*| = q_{\text{in}}/(1 + q_{\text{in}}) - r_{\text{in}}/(1 + r_{\text{in}})$, where q_{in} and r_{in} are the mass and the flux ratio in the inner pair. The wobble factors are negative when the subsystem belongs to the secondary component. If the inner subsystem is not resolved, one of the two parameters (semimajor axis a_{in} or wobble factor) must be fixed, and only the wobble amplitude (fa_{in} product) is constrained.

When the coverage of the orbit is partial, the data match a wide range of potential solutions. In such situations, I fix one or several elements to the values that match the estimated masses or other constraints after fitting the remaining elements. Thus, instead of exploring the full family of potential orbits, I select one member of this family that fits both the data and the additional constraints. Such tentative orbits still serve as references for wobble and usually give a good idea of the mutual orbit inclination Φ .

2.5. Description of the Tables

The main results of this work (orbital elements and observations) are condensed in three tables. Table 3 lists the orbital elements — visual, spectroscopic, or combined. The notations are standard: orbital period P , epoch of periastron T , eccentricity e , semimajor axis a (full or wobble), position angle of the ascending node Ω_A , longitude of periastron ω_A , inclination i , RV amplitudes of the primary and secondary, K_1 and K_2 , the systemic velocity V_0 , and the wobble factor f . When both positions and RVs are available, the elements match both, so ω_A is the periastron argument of the primary component and Ω_A is chosen to fit the position angles. The `orbit3` code always considers the inner subsystem as the primary component of the wide pair. When it is actually the secondary, the outer elements Ω_A and ω_A returned by the code are changed by 180° and the outer RV amplitudes are swapped.

Individual positions, their adopted errors, and residuals to the orbits are listed in Table 4, available in full electronically. The subsystems are identified by their WDS codes and components. Compared to the

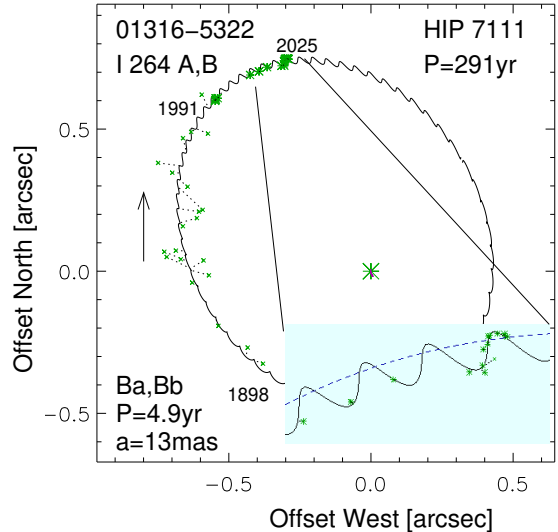


Figure 1. Orbits of HIP 7111. The outer trajectory with wobble (full line), SOAR observations (asterisks), and the center-of-mass trajectory (dashed line) plotted, with a zoomed fragment in the insert. Less accurate measurements are plotted as crosses.

published SOAR data, the positions are corrected for the small systematics determined in A. Tokovinin et al. (2022); in a few cases the speckle data are reprocessed. The second column indicates the subsystem; for example, A,B refers to the angle and separation between A and unresolved pair B, while A,Ba refers to the position of the resolved secondary Ba relative to A. The RVs and their residuals to orbits are listed in the electronic Table 5. Larger errors are assigned to some RVs to down-weight their impact on the orbit.

3. HIP 7111 (QUADRUPLE)

This is a visual triple system where the distant ($40''$) companion C has been identified by J. Herschel in 1836 (HJ 3444), and the closer pair A,B was discovered by R. Innes in 1898 (I 264). The Gaia astrometry of A and B, presently at $0''.8$ separation, is uncertain (parallaxes 10.61 and 8.83 mas, mean parallax 9.72 mas). The distance to the system is known from the accurate parallax of C, 9.677 ± 0.013 mas. Visual orbits of the A,B pair were computed by J. A. Munn et al. (2022) and A. Tokovinin et al. (2022), the latter has a period of 260 yr. The A,B pair was observed at SOAR frequently as a calibrator until the wobble in its motion became obvious (Figure 1). The fitted wobble orbit has a period of 4.9 yr and an amplitude of 12.8 mas, while the outer period is revised here to 291 yr. I assume that the subsystem belongs to star B because it has a larger RUWE in GDR3 (5.3 and 12.4 for A and B, respectively). The mass of Ba is $1.2 M_\odot$, the astrometric orbit gives a

Table 3. Orbital Elements

WDS	System	P	T	e	a	Ω_A	ω_A	i	K_1	K_2	V_0	f
HIP		(yr)	(yr)	($''$)	(degr)	(degr)	(degr)	(km s $^{-1}$)	(km s $^{-1}$)	(km s $^{-1}$)		
01316–5322	Ba,Bb	4.915	2023.96	0.595	0.0123	13.2	303.2	100.6	1.0
7111		± 0.037	± 0.13	± 0.120	± 0.0015	± 4.0	± 12.8	± 3.8	fixed
01316–5322	A,B	291.4	1845	0.30	0.639	28.5	164.1	148.2
7111		± 4.8	± 11	fixed	± 0.007	± 10.8	± 21.6	± 4.4
02460–0457	Ba,Bb	37.90	2000.41	0.570	0.141	51.0	35.8	30.3	-0.333
12912		± 0.66	± 0.67	± 0.063	fixed	± 19.7	± 21.0	± 5.4	± 0.029
02460–0457	A,B	1000	1898.4	0.334	1.551	146.3	46.0	126.9
12912		fixed	± 41.1	± 0.099	fixed	± 11.3	± 43.7	± 1.2
03496–0220	Ba,Bb	0.68749	2015.6334	0.4095	0.0185	55.8	343.9	99.5	20.608	23.970	...	-0.241
17895		± 0.00026	± 0.0012	± 0.0042	fixed	± 6.5	± 0.9	± 6.8	± 0.141	± 0.144	...	± 0.028
03496–0220	A,B	47.19	1989.57	0.607	0.365	67.1	285.1	122.9	5.88	4.52	6.34	...
17895		± 2.71	± 1.39	± 0.068	± 0.018	± 2.4	± 2.8	± 3.3	± 1.57	± 0.75	± 0.10	...
04218–2146	Aa,Ab	12.515	2025.587	0.206	328.2	...	4.214	...	-3.665	...
20375		± 0.235	± 0.060	± 0.012	± 2.6	...	± 0.078	...	± 0.099	...
08391–5557	B,C	23.47	2005.3	0.25	0.0728	173.7	263.0	155.0	-0.386
42424		± 1.08	± 1.9	fixed	± 0.0030	± 33.0	± 18.1	± 6.2	± 0.029
08391–5557	A,B	1100	1869.1	0.437	1.070	60.8	304.6	162.4
42424		fixed	± 18.1	± 0.049	fixed	± 83.9	± 70.2	± 9.8
10367+1522	B,C	8.584	2011.080	0.3398	0.1470	86.4	55.4	23.6	-0.500
...		± 0.019	± 0.023	± 0.0035	± 0.0008	± 2.7	± 2.6	± 1.0	± 0.006
10367+1522	A,B	120.0	2030.60	0.352	1.080	94.2	201.1	22.2
...		fixed	± 0.56	± 0.024	± 0.029	± 4.0	± 3.6	± 5.5
14040–4437	Aa,Ab	0.06569	2025.2692	0.6534	83.52	...	54.81	58.55
68717		...	± 0.0009	± 0.14	...	± 0.10	± 0.12
14040–4437	A,B	414	2288	0.620	1.007	127.4	277.4	62.8	2.30	4.20	-3.32	...
68717		± 28	± 21	fixed	± 0.060	± 2.4	± 2.3	± 1.2	fixed	fixed	± 0.04	...
15474–1054	Ba,Bb	0.3640	2018.0863	0.1125	220.3	...	15.193	13.649
77349		...	± 0.0025	± 0.0048	± 2.5	...	± 0.097	± 0.102
15474–1054	A,B	8.320	2014.972	0.4366	0.2429	95.7	49.6	116.3	7.197	6.671	2.975	...
77349		± 0.011	± 0.013	± 0.0027	± 0.0011	± 0.3	± 0.4	± 0.3	± 0.138	± 0.135	± 0.062	...
16161–3037	Aa,Ab	7.47	2019.42	0.266	0.0344	243.9	251.6	145.0	0.516
79076		± 0.14	± 0.96	± 0.090	± 0.0024	± 46.7	± 17.1	fixed	± 0.066
16161–3037	A,B	166.5	2086.3	0.141	0.323	166.6	124.0	150.1
79076		± 8.0	± 8.2	± 0.044	± 0.029	± 8.8	± 11.5	± 3.6
18250–0135	Aa,Ab	11.50	2022.56	0.90	0.0196	34.6	111.1	102.5	1.0
90253		± 0.12	± 0.10	fixed	± 0.0014	± 4.2	± 4.4	± 2.8	fixed
18250–0135	A,B	381.0	1890.6	0.578	0.678	175.7	44.5	93.3
90253		± 26.8	± 3.9	± 0.041	± 0.031	± 0.4	± 7.1	± 0.5
19540+1518	Aa,Ab	67.7	1956.14	0.695	0.262	102.7	164.8	142.4	0.476
97922		± 0.7	± 0.58	± 0.014	fixed	± 8.9	± 8.0	± 7.6	± 0.024
19540+1518	A,B	3100	1802.3	0.411	3.77	3.8	12.5	145.6
97922		fixed	± 31.8	± 0.030	fixed	1	± 15.1	± 12.2	± 2.7
20503–7502	Aa1,Aa2	0.04222	2025.3182	0.0296	333.2	...	41.74	47.55
102855		fixed	± 0.0002	± 0.0011	± 1.5	...	± 0.08	± 0.09
20503–7502	Aa,Ab	0.3533	2025.280	0.250	305.0	50.4	3.49	...	15.14	...
102855		fixed	± 0.013	± 0.017	± 15.7	fixed	± 0.30	...	± 0.22	...

mass of $0.6 M_\odot$ for Bb, and the full semimajor axis of the Ba,Bb orbit is 36 mas. The outer orbit is not fully constrained, so its eccentricity is fixed to $e_{A,B} = 0.3$. The outer orbit yields a mass sum of $3.4 M_\odot$, matching the estimated mass sum of three stars. Fitting the wobble leaves weighted residuals of 2.5 mas; they increase to 7 mas without wobble.

The ascending nodes of both orbits remain ambiguous, so the mutual inclination can be either 50° or 110° . The inner eccentricity of $e_{\text{Ba,Bb}} = 0.6$ provides indirect evidence of large mutual inclination and Kozai-Lidov cycles (S. Naoz 2016).

4. HIP 12912 (TRIPLE)

The visual binary WDS J02460–0457 (ADS 2111) has been resolved for the first time by S. W. Burnham in

Table 4. Position Measurements and Residuals (Fragment)

WDS	Syst.	Date	θ	ρ	σ_ρ	$(O-C)_\theta$	$(O-C)_\rho$	Method ^a
		(J2000)	(JY)	($^{\circ}$)	($''$)	($''$)	($''$)	
01316–5322	A,B	1986.8590	43.7	0.8600	0.0500	-1.0	0.0513	M
01316–5322	A,B	1990.9202	42.4	0.8120	0.0050	0.4	-0.0070	s
01316–5322	A,B	1991.2500	41.9	0.8170	0.010	-0.0	0.0006	H
01316–5322	A,B	1991.7119	42.3	0.8130	0.0050	0.5	-0.0003	s
01316–5322	A,B	1995.8566	41.5	0.8130	0.0100	2.4	-0.0086	s
01316–5322	A,B	2016.0000	27.1	0.8054	0.0020	-0.0	-0.0017	G
01316–5322	A,B	2021.8906	23.7	0.7883	0.0020	0.1	-0.0026	S

^a Methods: G: Gaia; H: Hipparcos; M: visual micrometer measurement; S: speckle interferometry at SOAR; s: speckle interferometry at other telescopes; V: adaptive optics at VLT.

Table 5. Radial Velocities and Residuals (Fragment)

WDS	Comp.	JD	RV	σ	$(O-C)$	Instr. ^a
	(J2000)	(JD – 24,00,000)	(km s^{-1})			
03496–0220	Ba	57257.8899	35.183	0.300	-0.675	CHI
03496–0220	Bb	57257.8899	-26.605	0.300	-0.558	CHI
03496–0220	Ba	57276.8025	27.717	0.300	0.226	CHI
03496–0220	Bb	57276.8025	-16.213	0.300	0.082	CHI

^a Instruments: CHI: CHIRON; LCO: DuPont echelle.

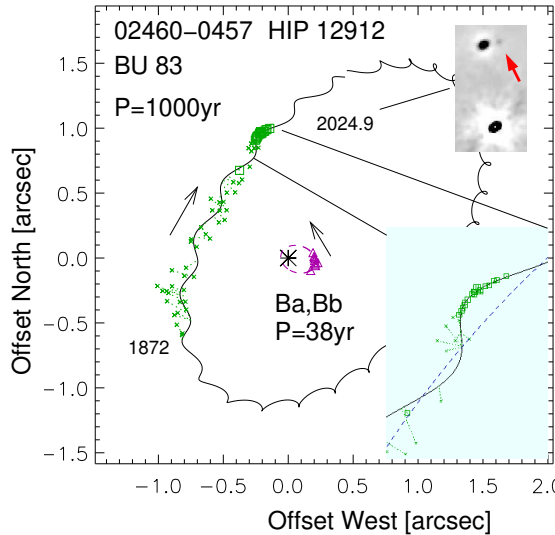


Figure 2. Orbits of HIP 12912. The inserts show a fragment of the speckle autocorrelation image taken in 2024.9 and the zoomed part of the outer orbit with the wobble (full line), SOAR observations (squares), and the center-of-mass trajectory (blue dashed line). Less accurate measurements are plotted by crosses. The magenta ellipse with triangles shows the inner orbit of Ba,Bb.

1872 (BU 83). Its monitoring during several decades revealed only a slow motion. However, [J. Dommangé \(1972\)](#) suspected a wave with a period of 36 yr, presumably caused by an inner subsystem. Resolution of the subsystem by speckle interferometry at SOAR was reported by [A. Tokovinin et al. \(2018\)](#). Originally, the subsystem was attributed to the brighter star A, but subsequent observations demonstrated that it belongs to the secondary star B. Here the updated analysis of this triple based on the observations till 2024.9 is presented. The inner period of 38 yr is confirmed. The outer orbit is poorly constrained, so the period of 1000 yr is imposed. Figure 2 shows the orbits and its zoomed segment demonstrating wobble in the motion of A,B. The wobble factor $f = -0.33 \pm 0.03$ implies the mass ratio $q_{\text{Ba,Bb}} = 0.49$. The weighted rms residuals in the outer positions are 4.5 mas with wobble and 14 mas without.

The magnitude difference between Ba and Bb is 3.25 ± 0.31 mag in the I filter (the companion is not detected in the y filter). The measurements of the inner pair in 2012–2024 cover only a fraction of its orbit, while the historic data for A,B are noisy. In this situation, additional constraints on the masses are helpful. By trial and error, I adopted masses of 1.41, 1.05 and $0.58 M_{\odot}$ for A, Ba, and Bb, respectively. The fluxes

of such stars derived from the 2.5 Gyr solar-metallicity isochrone (A. Bressan et al. 2012) match the combined and differential photometry. However, the inner mass sum of $1.63 M_{\odot}$ is less than predicted by the unconstrained fit. To remove the discrepancy, the inner semimajor axis is fixed at $0''.141$ without increasing the residuals. The outer semimajor axis is also fixed to match the target mass sum of $3.05 M_{\odot}$.

Although the inner and outer orbits are not well constrained, their large mutual inclination is incontestable, given the opposite motion directions. The two angles Φ computed from the orbits are 124° or 118° . Quasi-orthogonal orbits entail the von Zeipel-Kozai-Lidov cycles (S. Naoz 2016), hence the large inner eccentricity $e_{\text{Ba,Bb}} = 0.57$ is natural.

The GDR3 provided the 5-parameter astrometric solution for star A with a small RUWE of 0.9, and only the coordinates for star B (hence the relative position of A,B in GDR3 is suspect). No additional companions with common PM (CPM) within $2'$ are found in GDR3.

5. HIP 17895 (TRIPLE)

This nearby solar-type star has been resolved as a $0''.3$ pair in 2000 by E. P. Horch et al. (2002); it received the designation YR 23 in the WDS. In 2015, its first, still preliminary orbit was computed (R. L. Riddle et al. 2015), suggesting that the RV variation might be measurable. Meanwhile, double lines were noted by B. Nordström et al. (2004). The triple nature of this system was definitely revealed by N. A. Gorynya & A. Tokovinin (2018) who presented the 250-day orbit of the inner subsystem Ba,Bb. Spectra taken with CHIRON are triple-lined, allowing to measure the RVs of all three stars when the lines are not blended. The dip of A is broadened by axial rotation.

The semimajor axis of the inner orbit is 18.5 mas. As the masses and fluxes of Ba and Bb are slightly different, a wobble in the motion of A,B with an amplitude of 4 mas was expected. The YR 23 pair has been monitored at SOAR for detecting this wobble and improving the outer orbit; the results are presented here (Figure 3). The CHIRON spectrum taken in 2025.76 further constrains the RV amplitudes in the outer orbit. I do not include some published RVs from N. A. Gorynya & A. Tokovinin (2018) in Table 5.

The inner and outer orbits were fitted jointly. The inner subsystem is not resolved, so its axis was fixed to the computed value (18.5 mas). The wobble factor $f^* = -0.24 \pm 0.03$ corresponds to the amplitude of 4.4 mas. The weighted rms residuals of the speckle data are 1.3 mas. Without wobble, the residuals increase to 3 mas, so the astrometric effect of the inner

subsystem is detected reliably. The inner inclination is $i_{\text{Ba,Bb}} = 99.5 \pm 6.8^{\circ}$; it leads to the masses of 0.98 and $0.84 M_{\odot}$ for Ba and Bb, respectively. With the photometric mass of A, $1.14 M_{\odot}$, the outer mass sum is $2.96 M_{\odot}$. The outer orbit and the Hipparcos parallax of 19.63 mas correspond to the mass sum of $2.89 M_{\odot}$, in excellent agreement. However, the RV amplitudes in the outer orbit are not yet measured reliably; they give an outer mass sum of only $1.7 M_{\odot}$. The next periastron in 2036 gives an opportunity to measure better the RV amplitudes and other outer elements.

Both inner and outer orbits are relatively eccentric. The known orientation of the inner orbit and the correct outer node yield a mutual inclination of 26° , while the period ratio is ~ 69 .

6. HIP 20375 (TRIPLE)

The solar-type (G0V) star HIP 20375 (HD 27723) has been known as an unresolved binary for a long time, based on its astrometric acceleration (V. V. Makarov & G. H. Kaplan 2005) and a slightly variable RV (B. Nordström et al. 2004). Gaia DR3 detected both effects, providing a 9-parameter acceleration solution and a quadratic RV trend in the NSS catalog (Gaia Collaboration et al. 2023). Despite being relatively bright ($V = 7.54$ mag), this star does not have historic RVs useful for this study (the data of Nordström et al. are inaccessible). The faint (photometric mass $\sim 0.1 M_{\odot}$) CPM companion B at $76''.3$ makes this system triple.

This star has been placed on the CHIRON program in 2015.6. These 12 RVs covering a time span of 10.1 yr show a slow variation. A clue to the orbital period is provided by the fact that the PMA values in Hipparcos and GDR3 are similar (T. D. Brandt 2021). So, the 24.75 yr interval between these missions likely equals one or two periods. The RV data were approximated initially by an orbit with a fixed 12.4 yr period; the final orbit in Table 3 has a similar period, although its coverage is not yet complete. The CHIRON RVs cover the same time as the full Gaia mission (which will be released in DR5), but are more accurate. The three RVs computed from the Gaia RV trend solution show a systematic offset of -0.6 km s^{-1} ; they are plotted by crosses in Figure 4 and are not used in the orbit fit. Suspiciously, the quadratic term in the Gaia RV trend formula is 7.6 times less than its error. The mean RV published by B. Nordström et al. (2004), -6.2 km s^{-1} , matches the orbit approximately if it refers to ~ 1985 .

The CCF dip is appreciably widened, with an estimated projected rotation of $V \sin i = 19.4 \text{ km s}^{-1}$. Nevertheless, the rms residuals of CHIRON RVs are only

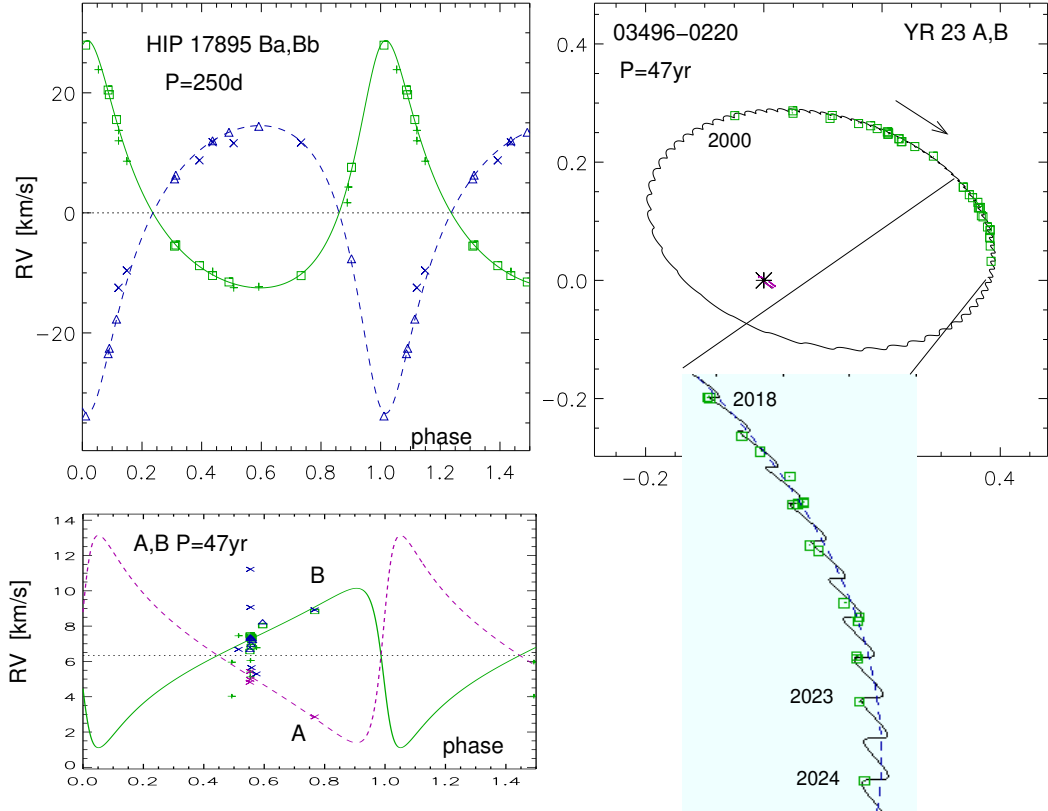


Figure 3. Orbit of HIP 17895. The inner and outer RV curves are shown on the left (less accurate RVs are plotted by pluses and crosses). In each plot, the motion in other subsystems is subtracted. The top-right panel shows the outer orbit on the sky, with the latest segment amplified in the insert.

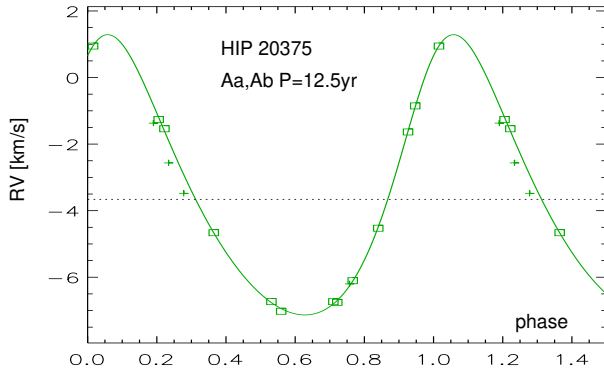


Figure 4. Spectroscopic orbit of HIP 20375. Three crosses denote RVs computed from the Gaia quadratic trend.

0.046 km s⁻¹. The lithium 6707Å line is not seen in the spectra, but an X-ray radiation from this system has been detected. Assuming a photometric mass of 1.2 M_{\odot} for Aa (spectral type F8V and $V - K = 1.28$ mag), the minimum mass of Ab is 0.45 M_{\odot} . Therefore, non-detection of its lines in the spectrum is natural. The semimajor axis of the Aa,Ab pair is 0''.12, so it is resolvable by adaptive optics; the estimated contrast in the K band is ~ 3.1 mag, while $\Delta I_{\text{Aa,Ab}} \sim 4.5$ mag is

beyond the limit of speckle-interferometric detection at close separations. This star was unresolved in the K and H bands at Gemini-S in 2011.85 (A. Tokovinin et al. 2012), when the separation was 44 mas (see below).

The two remaining unknown orbital elements can be adjusted to fit the PMAs in 1991.25 and 2016.0 reported by T. D. Brandt (2021); $\Omega = 239.5$ and $i = 65^\circ$ give a good match. The mass of Ab is then 0.51 M_{\odot} (spectral type M1.5V), $q_{\text{Aa,Ab}} = 0.43$, and $f = 0.30$ agrees nicely with the ratio of the orbital speed to the PMA. This indicates that Ab is a single star, rather than a close pair. The predicted position of Aa,Ab in 2026.0 is 233°7 and 0''.094. The pair will become closer in 2029 and will open up to 0''.14 in 2033.

7. HIP 42424 (TRIPLE)

The classical visual binary WDS J08391–5557 (HJ 1443AB) has been known since 1913. Its secondary component has been resolved into a 0''.09 pair B,C at SOAR in 2013. Now the inner pair has covered nearly half of its orbit, justifying its preliminary analysis. The outer orbit is not constrained by the observed arc of 54°; yet, the orbit of A,B with $P = 1447$ yr and $e = 0.845$ was published by I. S. Izmailov (2019). It corresponds to a mass sum of 126 M_{\odot} with the GDR3 parallax of

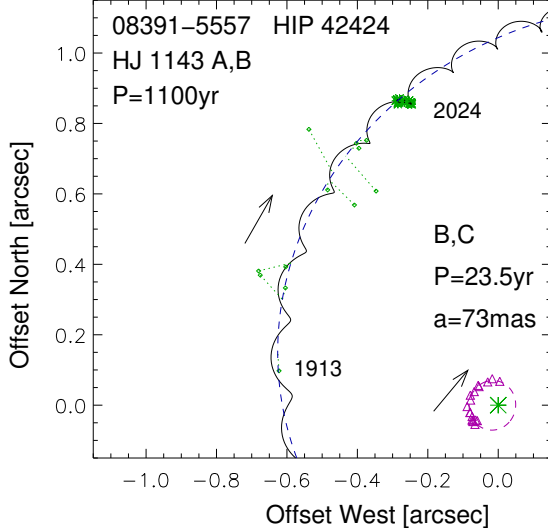


Figure 5. Orbits of HIP 42424. Magenta triangles and inner ellipse show the orbit of B,C.

6.22 ± 0.036 mas for star A. A more plausible (but still tentative) orbit with $P_{A,B} = 1100$ yr and $e_{A,B} = 0.44$ is proposed here. It serves, mainly, as a reference for measuring the wobble.

The two preliminary orbits are illustrated in Figure 5. The inner eccentricity was fixed at 0.25 because the free fit gives $e_{B,C}$ with a large error. The less certain outer period and semimajor axis were also fixed to values that match the observations and the estimated outer mass sum of $4.5 M_{\odot}$. The photometric masses of B and C, 1.48 and $1.08 M_{\odot}$, match approximately the inner mass sum of $2.9 M_{\odot}$ deduced from the orbit and the inner mass ratio of 0.64 inferred from the wobble factor $f = -0.39 \pm 0.03$. Both inner and outer pairs are seen nearly face-on and move clockwise; their two possible mutual inclinations are between 24° and 30° .

Gaia DR3 provides astrometric solutions for star A and the unresolved pair B,C. Their relative position, however, deviates from the center-of-mass orbit by -10° ; it is not used in the orbit fit. The inner orbit can be improved in the future if the speckle monitoring continues for another decade.

8. DAE 3 (TRIPLE)

This low-mass triple WDS J10367+1522 (UCAC4 527-051290) has been discovered by S. Daemgen et al. (2007) in 2006 using adaptive optics in a survey of young M-type dwarfs. Lacking common identifiers such as Hipparcos, it is referred to here by its WDS name DAE 3. The GDR3 parallax of 49.98 ± 0.09 mas places the system within 20 pc from the Sun. This triple system has been monitored at SOAR in 2017–2025. Additional data come from the literature, including accurate positions

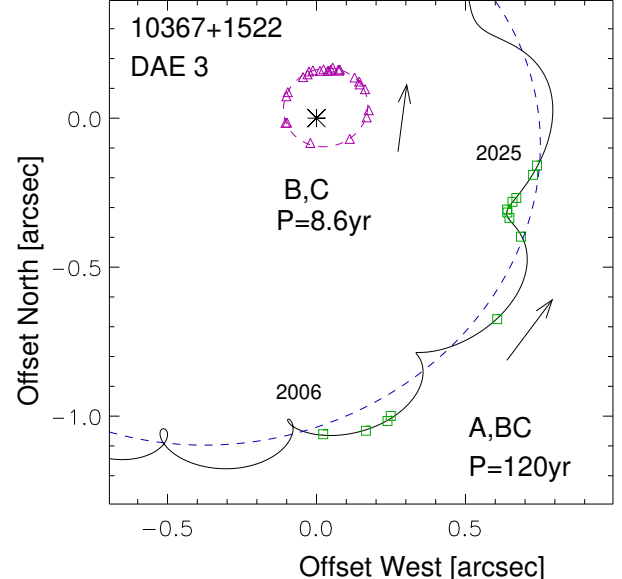


Figure 6. Orbits of DAE 3 (WDS J10367+1522).

from P. Calissendorff et al. (2022). Their orbit of B,C is very close to its present update, which benefits from six more years of data. This accurate orbit and the parallax give the inner mass sum of $0.344 M_{\odot}$, so the two equal-magnitude stars B and C are $0.172 M_{\odot}$ each. The wobble factor of -0.500 ± 0.006 confirms the equality of the inner masses (Figure 6).

The 67° arc of the outer orbit covered by the measurements gives only loose constraints, allowing periods from ~ 60 to ~ 250 years (234 yr in P. Calissendorff et al. 2022); the unconstrained fit yields $P_{A,B} = 120 \pm 34$ yr. The mass of star A estimated from its absolute magnitude $M_K = 7.06$ mag is about $0.29 M_{\odot}$ and corresponds to the spectral type M3.5V. Therefore, the outer mass sum should be around $0.63 M_{\odot}$. The outer period of 120 yr gives the outer mass sum of $0.70 M_{\odot}$, same as the 234 yr orbit of P. Calissendorff et al. (2022).

The enforced outer period of 120 yr makes the two orbits nearly coplanar, $\Phi = 6^\circ \pm 3^\circ$ (the alternative angle is 46°), while shorter or longer periods increase the derived mutual inclination. The planar architecture is common in low-mass triples, as well as equal masses in the inner and outer pairs (double twins). In the case of DAE 3, the inner mass ratio is indistinguishable from one, while the outer mass ratio depends on the mass of A ($0.29 M_{\odot}$ gives $q_{A,BC} = 0.84$). Continued monitoring of this remarkable low-mass triple system will eventually determine a reliable outer orbit, although the progress will be slow. Historic positions measured on photographic plates could, potentially, detect the photocenter motion with the expected amplitude of $\sim 0''.3$ and constrain the

outer period if the time base and accuracy of these positions are adequate.

9. HIP 68717 (QUADRUPLE OR QUINTUPLE)

The main component of this quadruple system of low-mass stars is known as HIP 68717, HD 122613, CPD-44 9060, and WDS J14040-4437. The outer 8'' pair AB,C was noted by [W. J. Hussey \(1915\)](#), and A,B has been resolved at 0''.6 by [R. T. A. Innes \(1911\)](#), although subsequent micrometer data revealed that this first measure was crude. More accurate positions were measured by Hipparcos in 1991 and by speckle interferometry at the Blanco and SOAR telescopes in 2008, 2009, and 2018. The arc of 57° covered by the position measures does not constrain the A,B orbit, and no orbit has been computed so far.

Gaia DR2 measured a parallax of 18.95 ± 0.78 mas for AB and 3.03 ± 0.96 mas for C. However, GDR3 gives only the positions of A and B without parallax and a parallax of 12.56 ± 0.23 mas for C, close to 11.76 ± 1.58 mas measured by Hipparcos for AB. The RVs of AB and C are -3.3 and -1.8 km s $^{-1}$, respectively. The GDR3 RUWE for C is elevated, 9.17, suggesting that it might contain an astrometric subsystem. The photometry of C ($V = 12.43$ mag, $K = 9.06$ mag) places it on the main sequence if its accurate GDR3 parallax is used, while AB is elevated above the main sequence because it contains three similar stars. There is little doubt that AB and C are physically related and that the discrepant astrometry is caused by the non-single nature of the sources.

[B. Nordström et al. \(2004\)](#) measured an RV of -4.0 km s $^{-1}$ twice over a time span of 2673 days and noted double lines. [A. Tokovinin et al. \(2015\)](#) observed AB and C with the DuPont echelle in 2008; they noted triple lines in the spectrum of AB and measured the RV of star C. Unfortunately, monitoring of the triple-lined star AB with CHIRON started only in 2025.

The lower-left panel of Figure 7 shows a typical triple-lined CCF computed from the CHIRON spectrum. The strongest central dip is identified here with the visual secondary B; its RV appears constant. The two weaker satellites belong to the double-lined spectroscopic binary Aa,Ab. The areas of the dips are 0.63, 0.45, and 0.33 km s $^{-1}$ for B, Aa, and Ab, respectively. Their sum for Aa+Ab is larger than for B, indicating a magnitude difference of 0.23 mag which agrees with 0.30 mag measured for A,B by Hipparcos and $\Delta I = 0.2$ mag measured at SOAR.

Frequent observations of AB with CHIRON in April-May 2025 allowed determination of the inner spectroscopic orbit with $P_{\text{Aa,Ab}} = 23.99489 \pm 0.00017$ days and $e_{\text{Aa,Ab}} = 0.6534 \pm 0.0009$. The periastron epoch is JD

24660744.5815 ± 0.0069 . The period and epoch in Table 3 are expressed in years, and their tiny errors are not listed there.

Splitting the combined flux of AB in proportion to the measured flux ratios and using the parallax of 12.56 mas leads to the photometric masses of 0.99, 0.93, and $1.04 M_{\odot}$ for Aa, Ab, and B, respectively. The mass sum of AB, $2.96 M_{\odot}$, helps to constrain its orbit. Another constraint is provided by the measured RVs and their change between 2008 and 2025. The RV amplitudes must match the estimated masses and the outer orbital elements. By trial and error, I found elements of the outer orbit with $P = 414$ yr which satisfy both the position measures and the additional constraints. A fixed eccentricity of $e_{\text{out}} = 0.62$ suffices to match the outer mass sum.

The final iteration on both orbits was made using `orbit3`. An offset of -0.5 km s $^{-1}$ was applied to the RVs measured in 2008 (it accounts for the zero-point), and errors of 0.5 km s $^{-1}$ were assumed for these RVs. The outer RV amplitudes of 2.3 and 4.2 km s $^{-1}$ are imposed to match the outer mass sum and the mass ratio, and the systemic velocity of -3.32 ± 0.04 km s $^{-1}$ is obtained from the fit. The RVs derived from blended CCFs (by fixing some dip parameters) are given low weights. The weighted rms residuals are 0.15, 0.20, and 0.04 km s $^{-1}$ for Aa, Ab, and B, respectively. Note that the relative position of A,B in GDR3 is discrepant and not used in the orbit fit. Owing to the small magnitude difference between A and B, they were likely swapped in some Gaia scans, as happened with other similar pairs.

The spectroscopic mass sum $M \sin^3 i$ of the inner pair is $1.57 M_{\odot}$, the photometric mass sum is $1.91 M_{\odot}$. Comparison of these numbers leads to the inclination $i_{\text{Aa,Ab}} = 70^\circ$ or 110° ; the outer inclination is $i_{\text{A,B}} = 62^\circ.3$. However, we do not know the direction of the inner motion and the position angle of the inner node, so the coplanarity between the orbits of Aa,Ab and A,B is possible, but not proven. The large inner eccentricity of 0.65 speaks against orbit alignment. The semimajor axis of the inner orbit, 2.5 mas, allows its resolution with VLTI to measure the relative inclination.

The outer companion C is currently separated from A by 7''.86, at a projected distance of 6.2 kau. The photometric mass of C is $0.69 M_{\odot}$, and the estimated period of AB,C is 8 kyr. Given that the Gaia astrometry of A and B is not reliable, I cannot compute the speed of C relative to AB. Furthermore, a potential subsystem Ca,Cb suggested by the large RUWE in GDR3 distorts the PM. If this subsystem exists, HIP 68717 is a hierarchical quintuple.

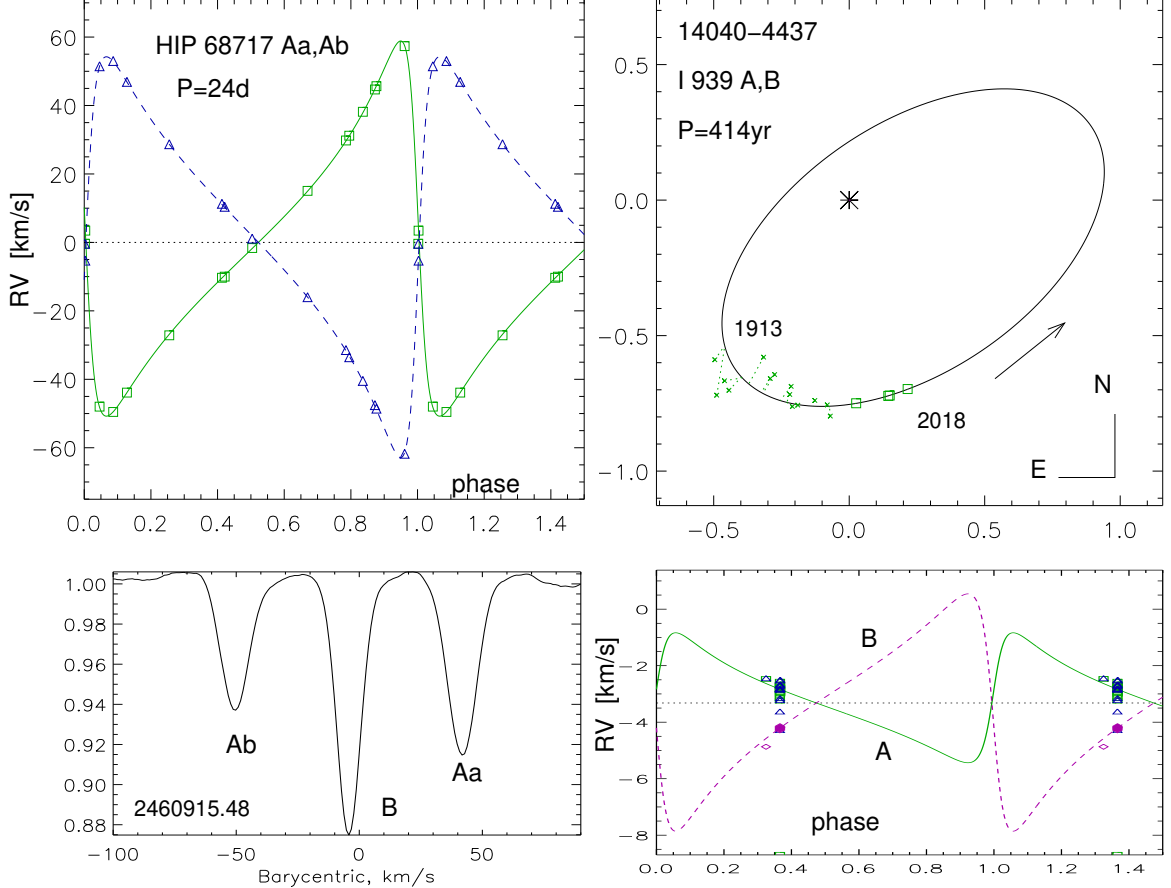


Figure 7. Orbits of HIP 68717: the inner RV curve (top left), the outer visual orbit, and the outer RV curve. The triple-lined CCF recorded on August 27, 2025 is shown.

The PM of AB (with the caveat mentioned above) and its RV correspond to the Galactic velocity of $(U, V, W) = (-4.8, -2.2, -5.4)$ km s $^{-1}$. The CHIRON spectrum does not contain the lithium 6707Å line or emissions. The projected rotation of three stars estimated from the width of CCF dips is between 6 and 8 km s $^{-1}$. Apparently this system belongs to the moderately old disk population. It is located on the sky in the direction of the Scorpius-Centaurus association, but is substantially closer to the Sun.

10. HIP 77349 (TRIPLE)

This nearby triple system WDS J15474–1054 is known as GJ 3916, LP 743-31, or G 152-50; the spectral type is M2.5V. The GDR3 does not give a 5-parameter astrometric solution, while Gaia DR2 measured a parallax of 62.52 ± 0.28 mas. The star has substantial literature. It has been placed on the CARMENES program of RV monitoring and was identified as a triple-lined system with periods of 132.959 and 3082 days by D. Baroch et al. (2021), who also computed the astrometric outer orbit based on the Hipparcos data. The multiplicity inferred from the space astrometry

prompted observations at SOAR, and the outer pair has been resolved in 2019 by E. H. Vrijmoet et al. (2022) at 0''.23 separation. Here the RVs from D. Baroch et al. (2021) are combined with the SOAR speckle data to derive two very well-constrained orbits.

Given that the RVs are published (they are not duplicated in Table 5), I do not plot here the inner orbit derived from the same data (it is listed in Table 3 only for completeness). The updated outer orbit using both positions and RVs is shown in Figure 8. The accuracy of 12 position measurements covering 5.65 yr is excellent, leaving residuals of 1.1 mas. The parallax of 62.52 mas corresponds to the outer mass sum of $0.848 M_{\odot}$, and the RV amplitudes give masses of 0.440 and $0.407 M_{\odot}$ for B and A, respectively (sum $0.847 M_{\odot}$). The agreement indicates that the Gaia DR2 parallax equals the orbital parallax. Furthermore, the known inner mass ratio $q_{Ba,Bb} = 0.90$ gives the directly measured masses of Ba and Bb, 0.208 and $0.232 M_{\odot}$ (Baroch et al. designated as Ba the less massive star in the inner pair, and I keep their choice). The spectroscopic inner mass sum of $0.323 M_{\odot}$ leads to the inner inclination of $64^{\circ}6$ or $115^{\circ}4$; the latter is close to the outer inclination of

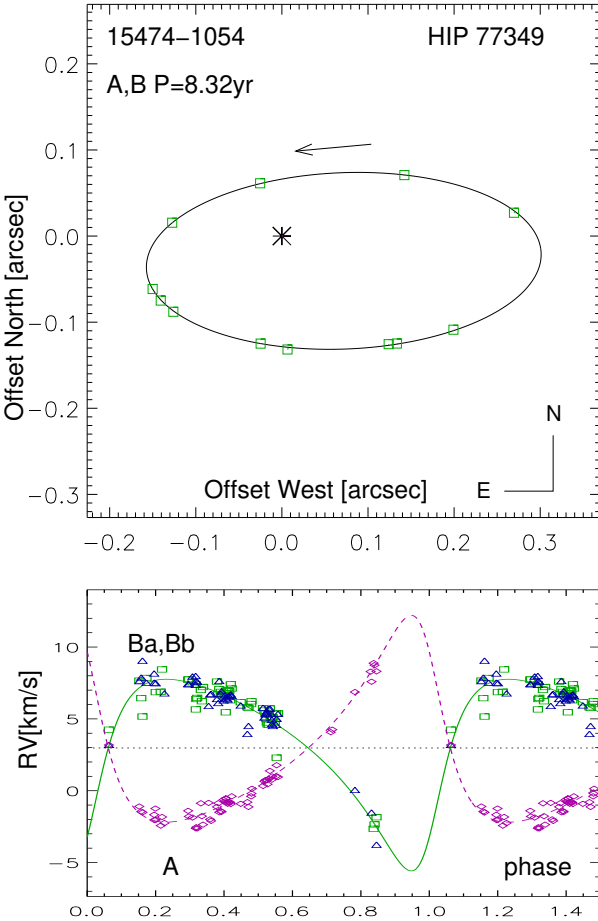


Figure 8. Outer orbit of HIP 77349 on the sky (top) and the RV curve (bottom), where diamonds, squares, and triangles indicate the RVs of A, Ba, and Bb, respectively (with subtracted Ba,Bb orbit).

$i_{A,B} = 116.3 \pm 0.3^\circ$, suggesting that the orbits could be coplanar. The semimajor axis of the inner pair Ba,Bb is 24.2 mas, making it resolvable at 8 m telescopes (at SOAR, a marginal elongation of the component B is suspected). Such a resolution would yield a direct measurement of the mutual inclination.

This relatively compact triple system composed of M-type dwarfs is a double twin with moderate eccentricities and, possibly, nearly coplanar orbits. Its resolution at SOAR, together with the triple-lined spectra, offered a unique opportunity to characterize the architecture almost completely. The masses are measured without any assumptions. However, a more elaborate treatment (including estimation of the confidence intervals) and interpretation of the masses and fluxes are outside the scope of this study.

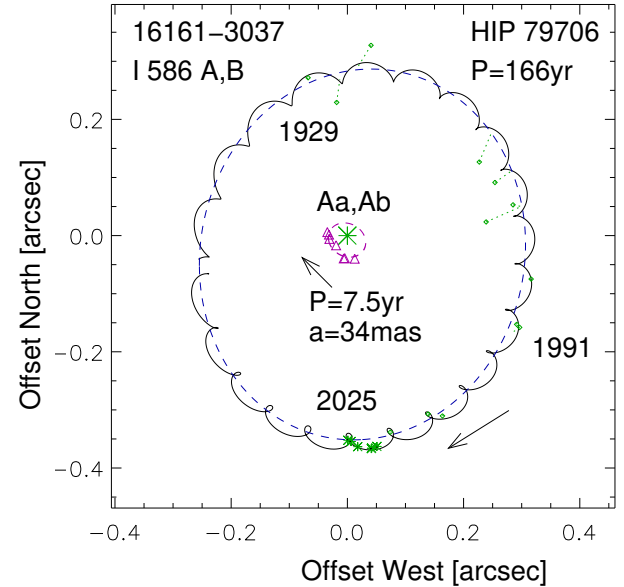


Figure 9. Orbits of HIP 79706.

11. HIP 79706 (TRIPLE)

The visual binary I 1586 AB (WDS J16161–3037) has been resolved for the first time at 0.5'' in 1927 by R. Innes. The CHARA group measured 3 accurate positions in 1983–2010 which, together with the Hipparcos, micrometer, and SOAR positions (2008–2025) define the outer 166 yr orbit rather well. Gaia DR3 did not resolve the A,B pair and measured a parallax of 6.20 ± 0.14 mas.

The tight (42 mas) inner pair Aa,Ab has been first noted in 2022.4, but, retrospectively, it can be seen in the data of 2018.2. Its separation is close to or below the diffraction limit of SOAR, making the measurements challenging (reference stars are always needed). By 2025, the Aa,Ab has apparently completed one full revolution, and an orbit with $P_{Aa,Ab} = 7.5$ yr is computed here (Figure 9). While the outer elements are measured without restrictions, the inner inclination of $i_{Aa,Ab} = 145^\circ$ was fixed (it is within the error bar of the unconstrained fit). The inner pair has a notable magnitude difference $\Delta I = 1.53 \pm 0.15$ mag and $\Delta y = 1.64 \pm 0.26$ mag. Yet, the wobble factor $f = 0.52 \pm 0.07$ suggests equal masses. Adopting the photometric masses of 1.67, 1.21, and 1.34 for Aa, Ab, and B, respectively, leads to the outer and inner mass sums of 4.2 and $2.9 M_\odot$. The parallax and the orbits give 5.1 and $3.1 M_\odot$. Considering the uncertainties, the agreement is acceptable.

The mutual inclination between the orbits is estimated to be either 37° or 50° , with a large uncertainty. A better angular resolution and accuracy (hence larger telescopes) are needed to improve the inner orbit. The inner

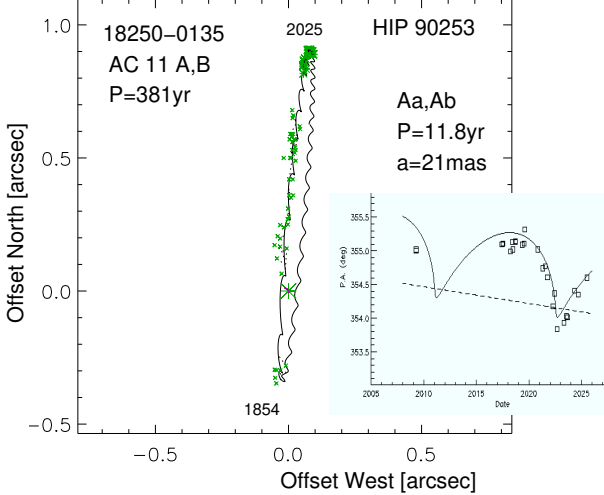


Figure 10. Orbit of HIP 90253 A,B with wobble. The insert shows position angles measured at SOAR vs. time (squares), while the solid and dashed lines depict orbits with and without wobble, respectively.

pair presently closes down and will become inaccessible to SOAR in the next few years.

12. HIP 90253 (TRIPLE)

The wobble in the observed motion of the SOAR calibrator binary WDS J18250–0135 (HIP 90253, HR 6898, AC 11, ADS 11324) has been suspected for several years. After 2023, the motion in position angle reversed its detection, furnishing a decisive proof (Figure 10). A tentative wobble orbit fitted to the positions jointly with the outer elements has a period of 11.8 yr and a large eccentricity of 0.90 (fixed). The inner pair spends most of the time near apastron, offset from the center of mass (the center-of-mass trajectory is plotted by the dashed line). The offset distorts the elements of the outer orbit, if not accounted for explicitly. The latest outer orbit computed without wobble (A. Tokovinin et al. 2022) had a period of 434 yr, revised here to 381 yr. This pair has been used for astrometric calibration of speckle instruments by several teams (e.g CHARA) and observed frequently for this reason; here I ignore speckle data from apertures less than 2 m as potentially inaccurate. Gaia DR3 did not measure the parallax, the DR2 parallax is 7.68 ± 0.17 mas, and the Hipparcos parallax is 7.49 ± 1.96 mas.

Comparison between Gaia DR2 and Hipparcos reveals a small PMA (T. D. Brandt 2018). This fact, together with the absence of the 5-parameter solution in GDR3, indicates that the subsystem causing wobble likely belongs to the brighter star A. The RV measurements found in the literature do not reveal any variability. Assuming that the subsystem belongs to star A, its full axis

is 61 mas, the masses of Aa and Ab are 2.3 and $1.6 M_{\odot}$, respectively (the F2V star Aa is slightly evolved), and the mass of AB is $5.8 M_{\odot}$; it matches approximately the outer mass sum derived from the orbit and the parallax. The wobble orbit is still tentative, it is not fully constrained. Two possible mutual inclinations, 139° or 40° , however uncertain, exclude mutual alignment and are in harmony with the large inner eccentricity.

13. HIP 97922 (QUADRUPLE)

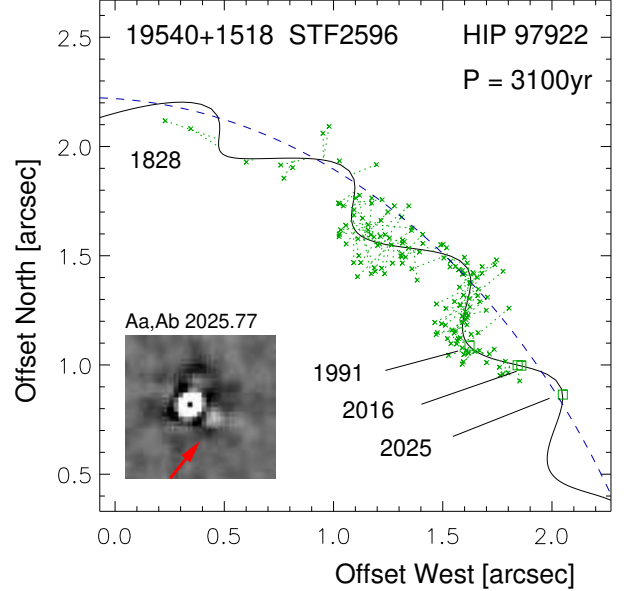


Figure 11. Outer orbit of HIP 97922. The squares and crosses show accurate and inaccurate measurements, respectively. The solid line is an orbit with wobble, and the blue dashed line is the center-of-mass trajectory. The insert shows fragment of the shift-and-add image of star A in the I filter with the inner companion Ab on the lower-right side at 0.092 separation.

The multiple system WDS J19540+1518 (HIP 97922, HD 188328, ADS 13082) consists of the outer pair A,B discovered by W. Struve in 1828 at $2''1$ separation (STF 2596) and the inner $0''.09$ pair Aa,Ab resolved in 2025.52 at SOAR and confirmed in 2025.77. A subsystem in the component A is detected independently by the elevated RUWE of 4.3 in GDR3 and by the PMA (T. D. Brandt 2021). The parallax of star B, 11.47 mas (distance modulus 4.70 mag) is adopted here; the parallax of A, 11.78 mas, could be slightly biased by the subsystem. The main star Aa of spectral type F8III is evolved.

A premature orbit of A,B with $P_{A,B} = 2971$ yr was derived by I. S. Izmailov (2019) by a formal fit to ~ 190 measures available in the WDS database. This orbit gives an implausible mass sum of $48 M_{\odot}$, while my estimate (including the subsystems) is $3.8 M_{\odot}$. Trying to

compute a more realistic outer orbit, I found that the historic measures show a clear wave with a period of ~ 60 yr. On the other hand, the $0''.09$ separation of Aa,Ab suggested a period around 13 yr. Using `orbit3`, I fitted the outer orbit with wobble that yields the expected mass sum (the data allow a wide range of outer orbits) and, at the same time, fits the position of Aa,Ab. The inner period of 67.8 ± 0.6 yr and the inner eccentricity of 0.70 are found; presently Aa,Ab is near the periastron, opening up slowly.

In 2025 October the main star A was reobserved at SOAR in the I and y filters to measure the magnitude difference $\Delta m_{\text{Aa,Ab}}$ (2.8 and 3.2 mag, respectively). Compared to the discovery measure three months earlier, the position angle of Aa,Ab decreased by 9° and the separation increased by 2 mas, in agreement with the inner orbit. The RV of 3.94 km s^{-1} measured with CHIRON in 2025 differs from 10.1 km s^{-1} measured by B. Nordström et al. (2004) around 1990.

The known period of Aa,Ab and the wobble amplitude lead to the conclusion that the new faint companion Ab is almost as massive as Aa, hinting that it could be a close pair. If so, eclipses might be found. Indeed, the TESS (G. R. Ricker et al. 2014) light curve shows a periodic signal with $P = 0.27$ day and an amplitude of 3.5%. Therefore, this star, known as a visual binary STF 26596 for two centuries, is in fact a quadruple system of 3+1 hierarchy.

Fitting both orbits proceeded iteratively. First, the obvious outliers were discarded, and most remaining micrometer measurements of A,B were assigned errors of $0''.1$. Speckle interferometry with moderate apertures in 1991–2014 is given errors of $0''.05$, while the Gaia and SOAR relative positions of A,B are given errors of 2 and 5 mas, respectively. As the outer orbit is not constrained, I fixed some of its elements during iterations, but finally kept only the period of 3100 yr fixed. The wobble amplitude of $0''.12$ is determined securely.

Figure 11 shows the fragment of the outer orbit constrained by the data, with a wave in the historic measurements. Note how the accurate measurements in 1991, 2015–2016, and 2025 (green squares) deviate from the center-of-mass motion depicted by the dashed line. The two orbits together predict the PM difference B–A of $(-17.6, -4.0)$ mas yr^{-1} in 2016, in reasonable agreement with the GDR3 PM difference of $(-18.3, -2.8)$ mas yr^{-1} . The PMA is $(-9.4, -1.0)$ mas yr^{-1} according to T. D. Brandt (2021) and $(-8.0, -0.5)$ mas yr^{-1} according to my orbits.

This star was monitored by TESS in sector 54 (June 2022); the data is available from the MAST archive (TESS Team 2021). The fragment of the light curve

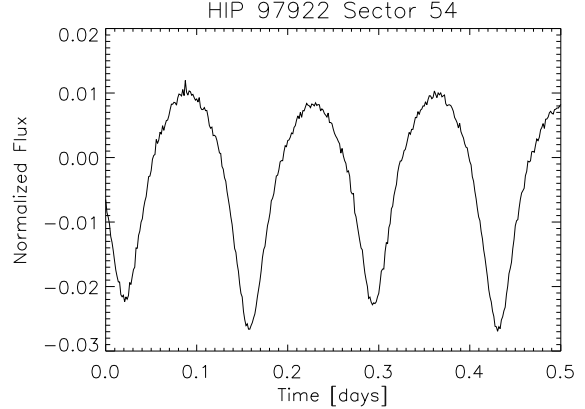


Figure 12. Fragment of the TESS light curve of HIP 97922. Deviations of the normalized flux from one are plotted vs. time.

Table 6. Photometry of HIP 97922

Band	m_A	$m_B - m_A$	Source
	(mag)	(mag)	
Hp	7.372	1.149	Hipparcos
430nm	7.841	1.277	Tycho
530nm	7.273	1.286	Tycho
G	7.097	1.426	Gaia DR3

plotted in Figure 12 is typical for contact eclipsing binaries. The two minima have a slightly different amplitude, so the true orbital period is $0^d 2730$. Short periods are found in other contact binaries, e.g. 44 Boo ($0^d 268$) and XY Leo ($0^d 284$). By the way, both these binaries belong to hierarchical systems.

The amplitude of the main minima is 3.5%. However, the light of Ab is diluted by the two brighter stars Aa and B contributing to the same TESS pixel. The true eclipse modulation amplitude is expected to be ~ 17 times larger, about 0.6 mag; it is typical for contact binaries of WMa type. The light curve resembles that of EK Com ($P = 0^d 2667$) from N. P. Liu et al. (2023). These authors determined physical parameters of several K-type binaries with comparably short periods; for EK Com they find masses of 1.02 and $0.28 M_\odot$ and the effective temperature of 5000 K. These parameters are adopted here as a proxy of our binary Ab1,Ab2. The standard relations between absolute magnitudes and periods of contact binaries (L.-Y. Song & Z.-J. Tian 2024) predict that Ab has an absolute M_G magnitude of ~ 5.3 mag, hence $G_{\text{Ab}} = 10.0$ mag, 2.9 mag fainter than Aa ($G_A = 7.10$ mag). This estimate agrees nicely with the measured magnitude difference of $\Delta I_{\text{Aa,Ab}} = 2.8$ mag.

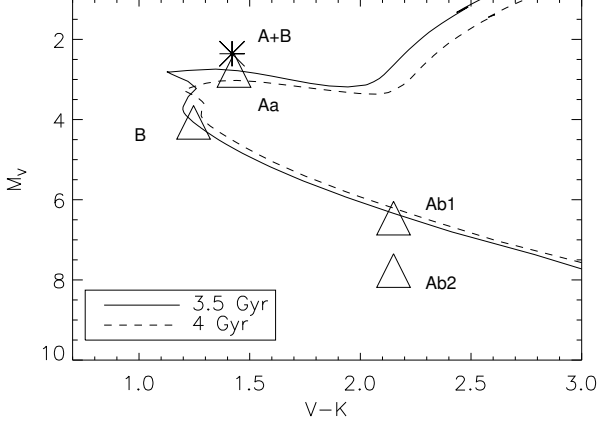


Figure 13. Tentative position of the components of HIP 97922 on the color-magnitude diagram (triangles). The asterisk denotes the combined flux of four stars. The lines are solar-metallicity PARSEC isochrones for the ages of 3.5 and 4 Gyr (A. Bressan et al. 2012).

Star Aa is evolved (F8III) and located well above the main sequence. The less evolved star B should be hotter. The resolved photometry of A and B collected in Table 6 confirms that the magnitude difference between A and B is smaller at shorter wavelengths. To model stellar parameters using constraints provided by the photometry, I tried first the age of 3 Gyr and assigned masses of 1.445 and $1.18 M_{\odot}$ to Aa and B, respectively. The component Ab is assumed to be 3.2 mag fainter than Aa in the V band, its flux is distributed between Ab1 and Ab2 in the 0.7:0.3 proportion, and the color $V - K = 2.15$ mag is assigned to match the Ab effective temperature of 5000 K (spectral type K2V), appropriate for a 0^d27 contact binary. The model predicts the combined system magnitudes in V and K 0.25 mag brighter than observed (7.06 and 5.64 mag, respectively). Increasing the age to 4 Gyr and adjusting the masses yields the system a bit too faint, and the best match is achieved for the age of 3.5 Gyr. Figure 13 shows the color-magnitude diagram. The triangles are placed on the isochrone for the adopted masses of Aa and B (1.343 and $1.12 M_{\odot}$), while the adopted parameters of Ab1 and Ab2 are used for the eclipsing pair. The 3.5 Gyr model yields total magnitudes of 7.15 and 5.73 mag in the V and K bands, respectively (0.1 mag fainter than observed), and the magnitude difference between A and B of 1.21 mag in B and 1.37 mag in I (compare to Table 6).

If the eclipsing binary EK Com is a proxy of Ab, its mass should be around $1.3 M_{\odot}$. The mass sum of Aa,Ab is therefore $\sim 2.6 M_{\odot}$, and the mass sum of A,B is $3.7 M_{\odot}$. In the final iteration on the orbits, I fixed both inner and outer semimajor axes to match the estimated mass sums. The wobble factor $f = 0.476 \pm 0.026$ implies

the inner mass ratio $q_{\text{Aa,Ab}} = 0.9 \pm 0.1$ and the Ab mass of $1.2 M_{\odot}$. The mutual inclination between outer and intermediate orbits is 52° or 45° . The orbit of the eclipsing pair must be highly inclined, hence it is also misaligned with the intermediate orbit having $i_{\text{Aa,Ab}} = 142^{\circ}$. Kozai-Lidov cycles in misaligned 3+1 quadruples could be at the origin of eclipsing pairs, as suggested by A. S. Hamers et al. (2015).

The adopted masses and orbits match all observational data reasonably well. However, the true parameters may differ. Further speckle monitoring of Aa,Ab will eventually yield the model-independent measurement of the inner mass sum and the inner mass ratio. The inner orbit predicts the RV amplitude of 3 km s⁻¹ for Aa, and the RV variation is indeed detected. This 3+1 quadruple system resembles WDS J01350–2955 (HIP 7372) containing a 0^d5 eclipsing pair BB Scl as secondary component in the intermediate pair with strong wobble. The discovery of the eclipsing pair in HIP 97922 was driven by the unexpectedly large wobble amplitude.

14. HIP 102855 (QUADRUPLE)

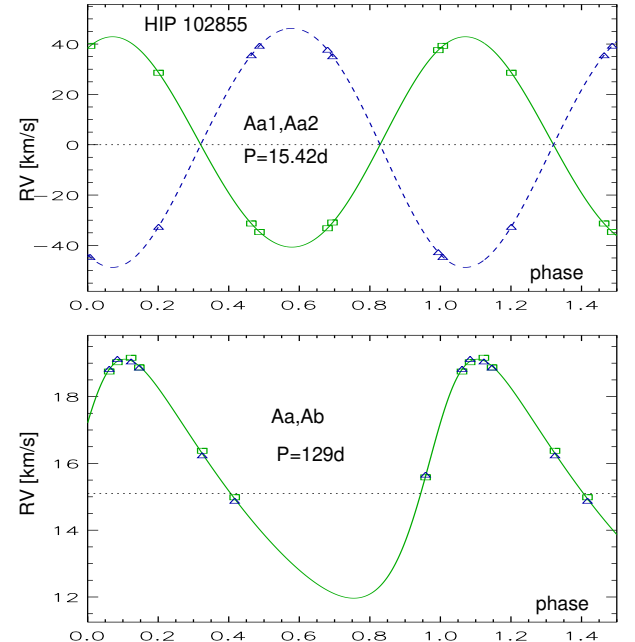


Figure 14. Spectroscopic orbits of HIP 102855 Aa1,Aa2 (top) and Aa,Ab (bottom). In each plot the contribution of other orbit is subtracted.

This inconspicuous 8th magnitude star (HD 197324, F7V) is featured in the Gaia NSS catalog twice: as a double-lined spectroscopic binary with a 15.4 day period and as an astrometric binary with a period of 129 days and a parallax of 8.29 mas. Some Gaia astrometric

orbits with such periods are spurious (cf. Figures 16 and 24 in [B. Holl et al. 2023](#)), so the veracity of this triple needed confirmation with CHIRON. Figure 14 shows a double-Keplerian fit to the RVs measured during 2025, where both periods are fixed to their respective NSS values owing to the small time span of our data. Both NSS solutions are confirmed; for example, the inner RV amplitudes of 41.74 and 47.55 km s⁻¹ resemble the NSS amplitudes of 39.65 and 49.13 km s⁻¹, while the inner eccentricity is small (0.030 CHIRON, 0.043 NSS). The systemic velocity of the inner pair varies with the 129 day period and an amplitude of 3.49 km s⁻¹. The outer eccentricity of 0.25 fitted to the RV curve is larger than $e = 0.14$ in the NSS astrometric orbit.

The ratio of CCF dip areas leads to the V magnitudes of 8.88 and 9.58 mag for Aa1 and Aa2, respectively, corresponding to the photometric masses of 1.31 and 1.06 M_{\odot} . The spectroscopic masses $M \sin^3 i$ are 0.60 and 0.53 M_{\odot} , hence the inner orbit has an inclination of 51° or 129°. The outer astrometric orbit is inclined at 50°.4. The mass of Ab estimated from its RV amplitude and inclination is 0.16 M_{\odot} , while the amplitude of the astrometric orbit corresponds to 0.19 M_{\odot} . The contribution of Ab to the total flux is negligible.

The GDR3 catalog contains a fourth component B with $G = 15.8$ mag at 6°03 separation and 240°.9 angle from A, with common PM and parallax. This companion has not been noted previously. Star B is also found in the 2MASS catalog; its estimated mass is 0.38 M_{\odot} , and the period P^* of A,B deduced from the projected separation of 727 au is 11 kyr.

The inner compact triple has a remarkably small period ratio of 8.37. The small inner eccentricity and similar inclinations suggest coplanarity. The low-mass tertiary Ab apparently formed in the circumbinary disc around Aa1,Aa2 and had no chance to accrete a substantial mass while migrating to its present-day short period. The growth of Ab could be prevented by another star B that formed in the outskirts of the disk and preferentially accreted the infalling gas.

15. SUMMARY

This work contributes orbit determinations in a dozen of field stellar hierarchical systems covering a wide range of parameters, from inner periods of several days (spectroscopic) to outer periods exceeding a millennium, where a short measured arc gives only a crude idea of the orbit. In such cases, the knowledge of masses and distances helps to narrow down the parameter space. Mutual inclinations are determined whenever possible.

The diversity of configurations and parameters is obvious even in this small sample (see Table 2). Triple M-

dwarfs are represented by WDS J10367+1522 (masses from 0.17 to 0.29 M_{\odot} , periods 8.6 and \sim 120 yr) and a slightly more massive WDS J15474–1054 (HIP 77349, periods 133 days and 8.3 yr). These systems are approximately coplanar (although the resolution of the inner pair in HIP 77349 is still lacking), with moderate eccentricities and near-unity mass ratios in both inner and outer pairs (double twins). Such architecture is rather common, e.g. in HIP 64836 (periods 5 and 30 yr, masses around 0.6 M_{\odot}) discussed in the previous paper of this series ([A. Tokovinin 2025b](#)) or the emblematic triple LHS 1070 (WDS J00247–2653) with periods of 17 and 83 yr. These low-mass systems presumably formed in relative isolation and did not accrete much mass beyond their parent cores. Their planar architecture could be driven by the angular momentum of the core.

An opposite case of misaligned and eccentric orbits is exemplified here by HIP 12912 with counter-rotating subsystems and inner eccentricity of 0.57 or by HIP 90253 with inner eccentricity of \sim 0.9. Characteristically, stars in these systems are more massive. The quadruple HIP 97922 (discovered by modern observations of a well-known, uninteresting visual binary) is also misaligned, relatively massive (1.34 M_{\odot} primary), and contains a contact inner binary. The preference of close binaries to be within multiple systems is a well-known fact (see discussion and references in [A. Tokovinin 2021a](#)). Such pairs cannot form too early (otherwise they would merge). Dynamics of misaligned triples and quadruples is a potential channel of forming close binaries via Kozai-Lidov cycles and tidal friction ([P. P. Eggleton & L. Kisselva-Eggleton 2006](#); [D. Fabrycky & S. Tremaine 2007](#); [S. Naoz 2016](#)).

This work illustrates typical problems of the multiple-star study. The main one is the lack of relevant observations. The WDS archive of historic micrometer measures is of invaluable help, but they are not available for newly discovered hierarchies, while the accuracy and reliability of old measures are way below modern standards. Archival RVs are even less frequent; by an unfortunate tradition, spectroscopists usually withhold their data until orbit publication, even when most targets are not binary or the periods are longer than the time span of their program (e.g. [B. Nordström et al. 2004](#)). The final Gaia data release 5 will be limited by the 11 yr duration of this mission and by the angular resolution of the 1 m Gaia aperture. The second problem is the complex and intertwined nature of orbital information encoded in the raw data. While the automatic pipelines occasionally fail in dealing with binaries, the failure rate for triples is expected to be even higher. The example of

successful Gaia orbits for the inner triple in HIP 102855 might be a lucky exception. So, targeted ground-based observations and a scrupulous individual treatment of each hierarchy are still be needed. This effort will be rewarded by a deeper understanding of stellar multiplicity.

ACKNOWLEDGMENTS

The research was funded by the NSF's NOIRLab. It is based on observations obtained at the Southern Astrophysical Research (SOAR) telescope, which is a joint project of the Ministério da Ciência, Tecnologia e Inovações do Brasil (MCTI/LNA), the US National Science Foundation's NOIRLab, the University of North Carolina at Chapel Hill (UNC), and Michigan State University (MSU). It is also based on observations at the 1.5 m telescope at CTIO operated by the SMARTS (Small and Moderate Aperture Research Telescope System) consortium. I thank operators of the 1.5 m tele-

scope for executing observations of this program and the SMARTS team for scheduling and pipeline processing.

This work used the SIMBAD service operated by Centre des Données Stellaires (Strasbourg, France), bibliographic references from the Astrophysics Data System maintained by SAO/NASA, and the Washington Double Star Catalog maintained at USNO. This work has made use of data from the European Space Agency (ESA) mission Gaia (<https://www.cosmos.esa.int/gaia>), processed by the Gaia Data Processing and Analysis Consortium (DPAC, <https://www.cosmos.esa.int/web/gaia/dpac/consortium>). Funding for the DPAC has been provided by national institutions, in particular the institutions participating in the Gaia Multilateral Agreement. This research has made use of the data collected by the TESS mission funded by the NASA Explorer Program; they were retrieved from the Barbara A. Mikulski Archive for Space Telescopes (MAST).

Facility: CTIO:1.5m, SOAR, Gaia

REFERENCES

Baroch, D., Morales, J. C., Ribas, I., et al. 2021, *A&A*, 653, A49, doi: [10.1051/0004-6361/202141031](https://doi.org/10.1051/0004-6361/202141031)

Brandt, T. D. 2018, *ApJS*, 239, 31, doi: [10.3847/1538-4365/aaec06](https://doi.org/10.3847/1538-4365/aaec06)

Brandt, T. D. 2021, *ApJS*, 254, 42, doi: [10.3847/1538-4365/abf93c](https://doi.org/10.3847/1538-4365/abf93c)

Bressan, A., Marigo, P., Girardi, L., et al. 2012, *MNRAS*, 427, 127, doi: [10.1111/j.1365-2966.2012.21948.x](https://doi.org/10.1111/j.1365-2966.2012.21948.x)

Calissendorff, P., Janson, M., Rodet, L., et al. 2022, *A&A*, 666, A16, doi: [10.1051/0004-6361/202142766](https://doi.org/10.1051/0004-6361/202142766)

Daemgen, S., Siegler, N., Reid, I. N., & Close, L. M. 2007, *ApJ*, 654, 558, doi: [10.1086/509109](https://doi.org/10.1086/509109)

Dommangé, J. 1972, *Bulletin of the Astronomical Observatoire Royale de Belgique*, 8, 63

Eggleton, P. P., & Kisseleva-Eggleton, L. 2006, *Ap&SS*, 304, 75, doi: [10.1007/s10509-006-9078-z](https://doi.org/10.1007/s10509-006-9078-z)

Fabrycky, D., & Tremaine, S. 2007, *ApJ*, 669, 1298, doi: [10.1086/521702](https://doi.org/10.1086/521702)

Gaia Collaboration, Brown, A. G. A., Vallenari, A., et al. 2021, *A&A*, 649, A1, doi: [10.1051/0004-6361/202039657](https://doi.org/10.1051/0004-6361/202039657)

Gaia Collaboration, Brown, A. G. A., Vallenari, A., et al. 2016, *A&A*, 595, A2, doi: [10.1051/0004-6361/201629512](https://doi.org/10.1051/0004-6361/201629512)

Gaia Collaboration, Arenou, F., Babusiaux, C., et al. 2023, *A&A*, 674, A34, doi: [10.1051/0004-6361/202243782](https://doi.org/10.1051/0004-6361/202243782)

Gorynya, N. A., & Tokovinin, A. 2018, *MNRAS*, 475, 1375, doi: [10.1093/mnras/stx3272](https://doi.org/10.1093/mnras/stx3272)

Hamers, A. S., Perets, H. B., Antonini, F., & Portegies Zwart, S. F. 2015, *MNRAS*, 449, 4221, doi: [10.1093/mnras/stv452](https://doi.org/10.1093/mnras/stv452)

Holl, B., Fabricius, C., Portell, J., et al. 2023, *A&A*, 674, A25, doi: [10.1051/0004-6361/202245353](https://doi.org/10.1051/0004-6361/202245353)

Horch, E. P., Robinson, S. E., Ninkov, Z., et al. 2002, *AJ*, 124, 2245, doi: [10.1086/342543](https://doi.org/10.1086/342543)

Hussey, W. J. 1915, *Publications of Michigan Observatory*, 1, 167

Innes, R. T. A. 1911 *Transvaal Observatory Circular*, 1, 61

Izmailov, I. S. 2019, *Astronomy Letters*, 45, 30, doi: [10.1134/S106377371901002X](https://doi.org/10.1134/S106377371901002X)

Liu, N. P., Qian, S. B., Liao, W. P., Huang, Y., & Yuan, Z. L. 2023, *AJ*, 165, 259, doi: [10.3847/1538-3881/acd04e](https://doi.org/10.3847/1538-3881/acd04e)

Makarov, V. V., & Kaplan, G. H. 2005, *AJ*, 129, 2420, doi: [10.1086/429590](https://doi.org/10.1086/429590)

Mason, B. D., Wycoff, G. L., Hartkopf, W. I., Douglass, G. G., & Worley, C. E. 2001, *AJ*, 122, 3466, doi: [10.1086/323920](https://doi.org/10.1086/323920)

Munn, J. A., Subasavage, J. P., Harris, H. C., & Tilleman, T. M. 2022, *AJ*, 163, 131, doi: [10.3847/1538-3881/ac41d2](https://doi.org/10.3847/1538-3881/ac41d2)

Naoz, S. 2016, *ARA&A*, 54, 441, doi: [10.1146/annurev-astro-081915-023315](https://doi.org/10.1146/annurev-astro-081915-023315)

Nordström, B., Mayor, M., Andersen, J., et al. 2004, *A&A*, 418, 989, doi: [10.1051/0004-6361:20035959](https://doi.org/10.1051/0004-6361:20035959)

Paredes, L. A., Henry, T. J., Quinn, S. N., et al. 2021, *AJ*, 162, 176, doi: [10.3847/1538-3881/ac082a](https://doi.org/10.3847/1538-3881/ac082a)

Pecaut, M. J., & Mamajek, E. E. 2013, *ApJS*, 208, 9, doi: [10.1088/0067-0049/208/1/9](https://doi.org/10.1088/0067-0049/208/1/9)

Raghavan, D., McAlister, H. A., Henry, T. J., et al. 2010, *ApJS*, 190, 1, doi: [10.1088/0067-0049/190/1/1](https://doi.org/10.1088/0067-0049/190/1/1)

Ricker, G. R., Winn, J. N., Vanderspek, R., et al. 2014, in Society of Photo-Optical Instrumentation Engineers (SPIE) Conference Series, Vol. 9143, Space Telescopes and Instrumentation 2014: Optical, Infrared, and Millimeter Wave, ed. J. Oschmann, Jacobus M., M. Clampin, G. G. Fazio, & H. A. MacEwen, 914320, doi: [10.1117/12.2063489](https://doi.org/10.1117/12.2063489)

Riddle, R. L., Tokovinin, A., Mason, B. D., et al. 2015, *ApJ*, 799, 4, doi: [10.1088/0004-637X/799/1/4](https://doi.org/10.1088/0004-637X/799/1/4)

Song, L.-Y., & Tian, Z.-J. 2024, *ApJ*, 961, 248, doi: [10.3847/1538-4357/ad12c0](https://doi.org/10.3847/1538-4357/ad12c0)

TESS Team. 2021, STScI/MAST, doi: [10.17909/T9-NMC8-F686](https://doi.org/10.17909/T9-NMC8-F686)

Tokovinin, A. 2014, *AJ*, 147, 87, doi: [10.1088/0004-6256/147/4/87](https://doi.org/10.1088/0004-6256/147/4/87)

Tokovinin, A. 2016, *AJ*, 152, 11, doi: [10.3847/0004-6256/152/1/11](https://doi.org/10.3847/0004-6256/152/1/11)

Tokovinin, A. 2017, Zenodo, doi: [10.5281/zenodo.321854](https://doi.org/10.5281/zenodo.321854)

Tokovinin, A. 2018a, *ApJS*, 235, 6, doi: [10.3847/1538-4365/aaa1a5](https://doi.org/10.3847/1538-4365/aaa1a5)

Tokovinin, A. 2018b, *PASP*, 130, 035002, doi: [10.1088/1538-3873/aaa7d9](https://doi.org/10.1088/1538-3873/aaa7d9)

Tokovinin, A. 2021a, *Universe*, 7, 352, doi: [10.3390/universe7090352](https://doi.org/10.3390/universe7090352)

Tokovinin, A. 2021b, *AJ*, 161, 144, doi: [10.3847/1538-3881/abda42](https://doi.org/10.3847/1538-3881/abda42)

Tokovinin, A. 2023, *AJ*, 165, 220, doi: [10.3847/1538-3881/acca19](https://doi.org/10.3847/1538-3881/acca19)

Tokovinin, A. 2024, *AJ*, 168, 190, doi: [10.3847/1538-3881/ad72e5](https://doi.org/10.3847/1538-3881/ad72e5)

Tokovinin, A. 2025a, *AJ*, 170, 143, doi: [10.3847/1538-3881/adee23](https://doi.org/10.3847/1538-3881/adee23)

Tokovinin, A. 2025b, *AJ*, 169, 124, doi: [10.3847/1538-3881/ada3c6](https://doi.org/10.3847/1538-3881/ada3c6)

Tokovinin, A., Fischer, D. A., Bonati, M., et al. 2013, *PASP*, 125, 1336, doi: [10.1086/674012](https://doi.org/10.1086/674012)

Tokovinin, A., Hartung, M., Hayward, T. L., & Makarov, V. V. 2012, *AJ*, 144, 7, doi: [10.1088/0004-6256/144/1/7](https://doi.org/10.1088/0004-6256/144/1/7)

Tokovinin, A., & Latham, D. W. 2017, *ApJ*, 838, 54, doi: [10.3847/1538-4357/aa6331](https://doi.org/10.3847/1538-4357/aa6331)

Tokovinin, A., Mason, B. D., & Hartkopf, W. I. 2010, *AJ*, 139, 743, doi: [10.1088/0004-6256/139/2/743](https://doi.org/10.1088/0004-6256/139/2/743)

Tokovinin, A., Mason, B. D., Hartkopf, W. I., Mendez, R. A., & Horch, E. P. 2018, *AJ*, 155, 235, doi: [10.3847/1538-3881/aabf8d](https://doi.org/10.3847/1538-3881/aabf8d)

Tokovinin, A., Mason, B. D., Mendez, R. A., & Costa, E. 2022, *AJ*, 164, 58, doi: [10.3847/1538-3881/ac78e7](https://doi.org/10.3847/1538-3881/ac78e7)

Tokovinin, A., Mason, B. D., Mendez, R. A., & Costa, E. 2024, *AJ*, 168, 28, doi: [10.3847/1538-3881/ad4d56](https://doi.org/10.3847/1538-3881/ad4d56)

Tokovinin, A., Pribulla, T., & Fischer, D. 2015, *AJ*, 149, 8, doi: [10.1088/0004-6256/149/1/8](https://doi.org/10.1088/0004-6256/149/1/8)

Toonen, S., Portegies Zwart, S., Hamers, A. S., & Bandopadhyay, D. 2020, *A&A*, 640, A16, doi: [10.1051/0004-6361/201936835](https://doi.org/10.1051/0004-6361/201936835)

van Leeuwen, F. 2007, *A&A*, 474, 653, doi: [10.1051/0004-6361:20078357](https://doi.org/10.1051/0004-6361:20078357)

Vrijmoet, E. H., Tokovinin, A., Henry, T. J., et al. 2022, *AJ*, 163, 178, doi: [10.3847/1538-3881/ac52f6](https://doi.org/10.3847/1538-3881/ac52f6)